Journal of Structural Geology 29 (2007) 1034–1048

JOURNAL OF STRUCTURAL GEOLOGY

www.elsevier.com/locate/jsg

Phenomenological modelling of crack generation in brittle crustal rocks using the particle simulation method

Chongbin Zhao [a,b,*], B.E. Hobbs [b], A. Ord [b], P.A. Robert [b], P. Hornby [b], Shenglin Peng [a]

[a] *Computational Geosciences Research Centre, Central South University, Changsha, China*
[b] *CSIRO Division of Exploration and Mining, P.O. Box 1130, Bentley, WA 6102, Australia*

Received 21 May 2006; received in revised form 4 February 2007; accepted 23 February 2007
Available online 12 March 2007

Abstract

The particle simulation method is used in this paper to explicitly simulate spontaneous crack generation in brittle crustal rocks. Although the method was previously used to simulate crack generation in small-scale laboratory specimens and mining sites, it has seldom been used to simulate spontaneous crack generation in large-scale geological systems. If a geological system can be treated as a quasi-static one, the mechanical response of the system should be independent of the loading rate. Based on this understanding, we have compared the commonly-used continuous loading procedure with a newly-proposed discontinuous loading procedure, which is independent of the loading rate within the elastic range of a particle system. The use of the discontinuous loading procedure enables the macroscopic elastic modulus of a two-dimensional particle system to be directly evaluated from the particle stiffness. However, the particle-size sensitivity analysis of at least two different models needs to be conducted for dealing with the particle size-dependent issue when the particle simulation method is applied to solve crack generation problems in geological systems. Through the phenomenological modeling of spontaneous crack generation problems, it has been demonstrated that the particle simulation method is useful for simulating spontaneous crack generation phenomena at geological length scales.

Keywords: Crack generation; Brittle rocks; Loading procedure; Particle simulation method; Discrete block mechanics

1. Introduction

Cracking and fracturing are one of the major failure mechanisms in brittle and semi-brittle materials. Since crustal materials of the Earth can be largely considered as brittle rocks, cracking and fracturing phenomena are ubiquitous in the upper crust of the Earth. For example, the study of rock fracturing in a complicated stress environment has, for many years, been an attractive topic for the fundamental understanding of earthquake mechanisms in the field of seismology and earthquake engineering. Many tectonic phenomena, such as propagation of oceanic rifts, magma intrusion due to hydraulic fracturing of rock masses, and generation of steeply dipping extensional cracks from the Earth's surface, are closely associated with cracking and fracturing of brittle rock masses. Since cracks and fractures are important channels to transport mineral-bearing fluids in porous rocks, the numerical simulation of a crack generation and propagation problem is equally important to the better understanding of the detailed ore-forming mechanism in a broad range of ore forming systems within the Earth's crust (Zhao et al., 1998, 2003, 2006a, 2007a).

Early studies on cracking and fracturing of brittle materials were based on the concept of fracture mechanics (Inglis, 1913; Griffith, 1920; Irwin and Washington, 1957), in which both the stress concentration caused by sharp-tipped flaws (i.e. small cracks) and the corresponding conditions for propagating these flaws were well investigated. Due to the limitations of analytical and computational tools, fracture mechanics at its early stage was mainly aimed at answering the scientific question related to when a fracture occurs rather than how it occurs.

* Corresponding author. Computational Geosciences Research Centre, Central South University, Changsha, China.
E-mail address: chongbin.zhao@iinet.net.au (C. Zhao).

0191-8141/$ - see front matter © 2007 Elsevier Ltd. All rights reserved.
doi:10.1016/j.jsg.2007.02.012

If the stress intensity factor at the tip of a crack is equal to or greater than the fracture toughness of the material, the crack becomes unstable and propagates at a speed near that of the transverse sound wave in the homogeneous linear elastic material until the stress intensity factor at the tip of the crack reaches a new stable state. The resulting crack in this case is often called the catastrophic crack.

However, because of the limitation of the conventional finite element method (which is usually based on the continuum mechanics) in simulating a large number of spontaneously generated cracks, the particle simulation method, such as the distinct element method that is implemented in a particle flow code (Cundall and Strack, 1979; Cundall, 2001; Itasca Consulting Group Inc., 1999; Potyondy and Cundall, 2004), provides a very useful tool to deal with this particular kind of problem. Due to the easy consideration of displacement discontinuities at a contact between two particles, the formulation based on the discrete particle simulation is conceptually simpler than that based on the continuum mechanics, because crack generation at a contact between two particles is a natural part of the particle simulation process.

The particle simulation method (e.g. the distinct element method) has been successfully used to solve a wide range of scientific and engineering problems such as those associated with soil/rock mechanics and geotechnical engineering (Cundall and Strack, 1979; Bardet and Proubet, 1992; Hazzard et al., 2000; Hazzard and Young, 2000; Cundall, 2001; Potyondy and Cundall, 2004; Klerck et al., 2004; Owen et al., 2004; McBride et al., 2004; Schubert et al., 2005; Zhao et al., 2006b), and those associated with geological and geophysical problems in both two and three dimensions (Saltzer and Pollard, 1992; Antonellini and Pollard, 1995; Donze et al., 1996; Scott, 1996; Strayer and Huddleston, 1997; Camborde et al., 2000; Iwashita and Oda, 2000; Finch et al., 2003, 2004; Strayer and Suppe, 2002; Burbidge and Braun, 2002; Imber et al., 2004). In particular, Finch et al. (2003, 2004) used distinct element modeling to investigate the contractional and extensional fault-propagation folding above rigid basement blocks. Strayer and Suppe (2002) used the distinct element method to simulate the out-of-plane motion of a thrust sheet during along-strike propagation of a thrust ramp. Burbidge and Braun (2002) employed the distinct element method to investigate the evolution of accretionary wedges and fold-and-thrust belts within the upper crust of the Earth. Imber et al. (2004) used the three-dimensional distinct element modeling to simulate the relay growth and breaching along normal faults. Although the particle simulation method was successfully used to solve many large-scale geological problems, little work, if any, has been reported on using the particle simulation method to deal with spontaneous crack generation problems in the upper crust of the Earth. However, the particle simulation method has been developed and used to simulate microscopic crack generation in small-scale laboratory specimens and mining sites (Itasca Consulting Group Inc., 1999; Potyondy and Cundall, 2004; Zhao et al., 2006b). Since both the time-scale and the length-scale are quite different between laboratory specimens and geological systems, it is necessary to apply the particle simulation method for solving spontaneous crack generation problems in the upper crust of the Earth.

If a geological system can be treated as a quasi-static one, then the mechanical response of the system should be independent of time so that the system response is loading-rate independent. Based on this understanding, we have examined the continuous loading procedure that is often used in PFC2D and a newly-proposed discontinuous loading procedure, which is independent of the loading rate, especially in the elastic response range of a particle system (Zhao et al., 2007b).

2. Concept and loading procedure of the particle simulation method

The central concept of the particle simulation method is that brittle rocks are assumed to be made up of many solid particles of different shapes and sizes. Each particle is connected through contact points with its neighboring particles. Interaction forces between any two particles are transferred through their contacts. This means that the mechanical properties of a particle are represented by the lumped mechanical parameters at its contacts with other particles. The useful lumped mechanical parameters are the normal and tangential stiffness of a particle. Since the normal stiffness and tangential stiffness are used to reflect the deformation characteristics of a particle, they are usually directly proportional to the elastic modulus of the particle system. In order to simulate tensile and shear failures at a contact between two particles, both the normal bond (representing the tensile strength) and the shear bond (representing the shear strength) are introduced in the particle simulation method (Wang et al., 2000; Delenne et al., 2004). The motion of each particle is described by the Newton's second law. Contact forces at a contact between two particles are calculated using a linear or non-linear relationship between force and relative displacement at this contact. If a particle is in contact with a boundary of the system, the contact force between the particle and the boundary can be calculated in exactly the same way as mentioned above, except for replacing the contacted neighboring particle by the contacted boundary. The total forces exerted on a particle are equal to the summation of all its contact forces at all contact points with other particles and boundaries of the system. The above concept was initially proposed in the distinct element method (Cundall and Strack, 1979; Cundall, 2001; Itasca Consulting Group Inc., 1999; Potyondy and Cundall, 2004) and it has been recently enhanced and implemented in the two-dimensional particle flow code (i.e. PFC2D).

A fundamental assumption associated with the distinct element method is that a quasi-static problem can be turned into an artificial dynamic problem, so that the explicit dynamic relaxation method is used to obtain the quasi-static solution from solving the artificial dynamic problem. In addition, the distinct element method is based on the idea that the time step used in the simulation is chosen so small that force, displacement, velocity and acceleration cannot propagate from any particle farther than its immediate neighbors during a single time step (Potyondy and Cundall, 2004). The servo-control technique (Itasca Consulting Group Inc., 1999) is often used to apply the equivalent velocity of applied stresses or forces to the loading boundary of the particle model. This posed an important scientific question: Is the mechanical response of a particle model dependent on the loading procedure to apply ''loads'' at the loading boundary of the particle model? Although this question was theoretically discussed in a recent publication (Zhao et al., 2007b), it needs to be investigated numerically in detail in this paper. If the mechanical response of a particle model is independent of the loading procedure, then this issue can be neglected when the application range of the particle simulation method is extended from a small-scale laboratory test to a large-scale geological problem.

To illustrate the ''load'' propagation mechanism associated with the distinct element method that is implemented in PFC2D, a one-dimensional idealized model consisting of ten identical particles is considered in Fig. 1. The model is in a rest state at the start of the simulation (i.e. at $t = 0$). It is assumed that each particle is simulated as a circular disk of unit thickness. Because the main purpose of this simulation is only to illustrate the ''load'' propagation mechanism, the normal contact stiffness and density of all the particles are assumed to be 2.0 KN/m and 1273.24 kg/m^3 respectively. The radii of all the particles are assumed to be 0.5 m, resulting in a mass of 1000 kg for each individual particle. Since two particles are connected in series, the total contact stiffness between any two particles is equal to 1.0 KN/m in this simulation. Although the ''load'' can be either a directly-applied force or an indirectly-applied force due to the constant velocity of a loading boundary, a directly-applied force of 100 N is considered in this idealized conceptual model. Damping is neglected, while the critical time step (Itasca Consulting Group Inc., 1999) is used, so that $\Delta t = \Delta t_{\mathrm{critical}} = \sqrt{m/k} = 1\mathrm{s}$ in the computation. Note that m stands for the mass of a particle, while k stands for the normal contact stiffness between any two particles. What we need to emphasize here is that when a ''load'' is applied to a particle system, what is the appropriate time to record the correct response of the whole system due to this ''load''? This issue is important due to the fact that the particle-scale material properties are only considered in a particle model and that a biaxial compression test is often used to determine the macroscopic material properties of the particle model.

Since the ''load'' applied to the first particle of this idealized model can be viewed as a dynamic disturbance, it will propagate at the rate of one particle per time step, as clearly demonstrated by the simulation result. The reason for this is that if damping is neglected and horizontal movement is only considered in this idealized model, the displacement of particle α at a given time can be essentially calculated using the following formulas (Itasca Consulting Group Inc., 1999).

$$\left(\frac{\mathrm{d}x_\alpha}{\mathrm{d}t}\right)^{t+\Delta t/2} = \left(\frac{\mathrm{d}x_\alpha}{\mathrm{d}t}\right)^{t-\Delta t/2} + \left(\frac{F^t_{\alpha x}}{m_\alpha}\right)\Delta t \tag{1}$$

$$x_\alpha^{t+\Delta t} = x_\alpha^t + \left(\frac{\mathrm{d}x_\alpha}{\mathrm{d}t}\right)^{t+\Delta t/2}\Delta t \tag{2}$$

$$u_\alpha^{t+\Delta t} = u_\alpha^t + \Delta u_\alpha^{t+\Delta t} = u_\alpha^t + \left(x_\alpha^{t+\Delta t} - x_\alpha^t\right) \tag{3}$$

where x_α^t and $x_\alpha^{t+\Delta t}$ are the horizontal coordinates to express the position of particle α at the time of t and $t+\Delta t$; m_α is the mass of particle α; $F^t_{\alpha x}$ is the total horizontal force exerted on particle α at the time of t; u_α^t and $u_\alpha^{t+\Delta t}$ are the horizontal displacements of particle α at the time of t and $t+\Delta t$; Δt is the time step in the computation.

Because the mass and the normal stiffness coefficient between any two particles have the same values respectively, the displacement of particle 1 (i.e. the particle with ''load'' P) is $D_1 = P\Delta t^2/m = 100 \times 1^2/1000 = 0.1\mathrm{m}$ at the end of the first time step (i.e. $t = 1\,\Delta t$, where Δt is the time step). The displacement obtained from this theoretical consideration is exactly the same as that obtained from the numerical particle simulation. Note that D_1 is the displacement of particle 1, while arrows show the displacements of each individual particle simulated in Fig. 1. Because the critical time step (Itasca Consulting Group Inc., 1999) is used in the computation, namely $\Delta t = \Delta t_{\mathrm{critical}} = \sqrt{m/k}$, the displacement of particle 1 (i.e. the particle with ''load'' P) can be theoretically expressed as $D_1 = P/k$ at the end of the first time step (i.e. $t = 1\Delta t$). The simulation results clearly show that, as expected, the ''load'' can only propagate from a particle to its immediate neighboring particles within a single time step. Thus, during the first time step, other nine particles in the right part of the model remain at rest. Obviously, the ''load'' propagates through the whole system at the end of $t = 10\,\Delta t$, resulting in a displacement of $D_1 = 10P/k = 1.0\mathrm{m}$ for particle 1.

It needs to be pointed out that in the distinct element simulation of this idealized system, there are two wave propagations. One is the simulated wave propagation, which moves one particle size per time step. The other is the physical wave propagation, determined by $\Delta t_{\mathrm{critical}} = \sqrt{m/k}$. Generally, for the sake of ensuring the numerical stability in complicated particle simulations, the simulated wave propagation should be quicker than the corresponding physical wave propagation, so that $\Delta t < \Delta t_{\mathrm{critical}} = \sqrt{m/k}$. For the purpose of illustrating the force propagation mechanism within this idealized system, we use $\Delta t = \Delta t_{\mathrm{critical}} = \sqrt{m/k}$, implying that the simulated wave propagation is comparable to the physical wave propagation, which results in an exact solution for the distinct element simulation of this idealized system.

At this stage, it is interesting to investigate the speed at which the elastic stress (strain) wave propagates in this idealized model. Clearly, the corresponding wave speed can be expressed as $C_{\mathrm{simulation}} = D/\Delta t_{\mathrm{critical}}$, where D is the diameter of the particles. Again, it is assumed that all the particles in the idealized model have the same diameters. For this idealized model, we have $E = k$ and $m = 1/4\rho\pi D^2$, where E is the elastic modulus of the particle material and ρ is the density of the particle material. This results in a wave speed of $C_{\mathrm{simulation}} = \sqrt{4/\pi}\sqrt{E/\rho} = \sqrt{4/\pi}C_{\mathrm{p}}$, where C_{p} is the P-wave speed of the

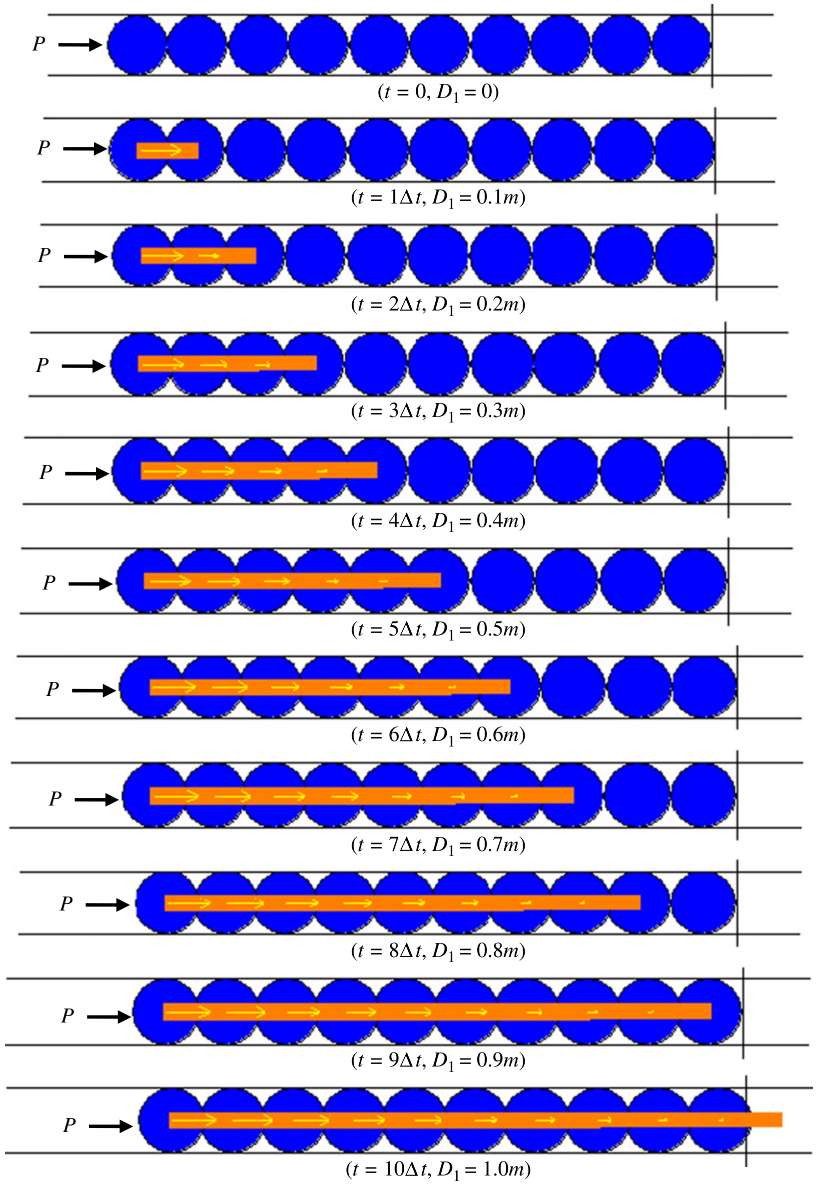

Fig. 1. Simulated force propagation in a ten-particle system at different time instants. The orange line shows the contact force between particles, while yellow arrows show the displacements at the mass centers of particles.

particle material. This indicates that the elastic wave energy (which transmits the applied load through the idealized model) propagates at a wave speed, which is a little higher than the P-wave speed.

If this one-dimensional idealized model is comprised of n particles of equal normal stiffness and mass, then the displacement of particle 1 (i.e. the particle with ''load'' P) is nP/k at the end of $t = n\,\Delta t$. This means that if one uses the record of the ''load'' and displacement at the end of the immediate loading step to determine the elastic modulus of this one-dimensional idealized particle system, then the determined elastic modulus will be exaggerated to n times, demonstrating that the continuous loading procedure (see Fig. 2) may be inaccurate when it is used with PFC2D to conduct the laboratory specimen test. This is because it is impossible to take the correct record of the ''displacement'', just at the end of a ''load'' increment. In other words, when a ''load'' increment is applied to the particle system, it must take a considerable number of time steps for the system to reach a quasi-static equilibrium state. It is the displacement associated with the quasi-static equilibrium state that represents the correct displacement of the system due to this particular ''load'' increment. To solve this problem, a newly-proposed discontinuous loading procedure is used in this paper (Zhao et al., 2007b). The discontinuous loading procedure (see Fig. 2) is comprised of two main types of periods, a loading period and a frozen period. In the loading period, a velocity increment is applied to the loading boundary of the system, while in the frozen period the loading boundary is fixed to allow the system to reach a quasi-static equilibrium state after a considerable number of time steps. This ensures that the potentially-induced momentum due to the decelerations and accelerations associated with the

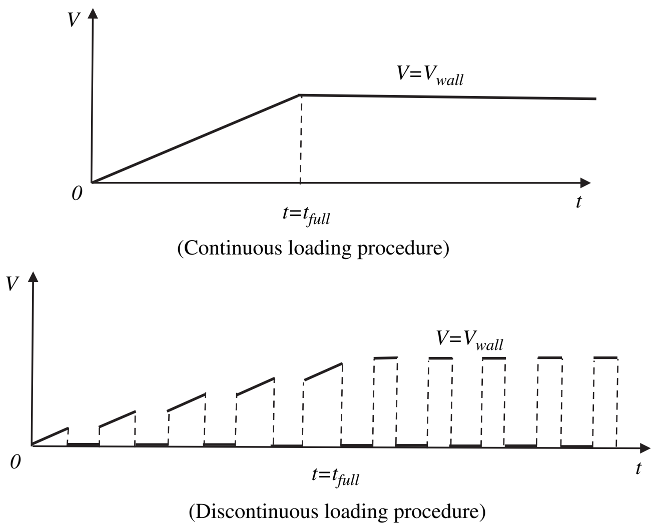

Fig. 2. Illustration of continuous and discontinuous loading procedures implemented in the particle simulation. V and V_{wall} are the loading rate and designed loading rate at the loading boundary of a particle system, respectively. t is the simulation time step, while t_{full} is the time step when the loading rate reaches the designed loading rate at the loading boundary of a particle system.

discontinuous loading procedure can be died out before the solution is considered as converged. It needs to be pointed out that a pair of load and displacement (or stress and strain) is correctly recorded at the end of a frozen period (Zhao et al., 2007b).

Compared with the finite element method with automatic re-meshing algorithms (Zienkiewicz and Zhu, 1991; Bouchard et al., 2003), the particle simulation method has the following four main advantages, at least from the crack-generation simulation point of view. Firstly, since there is no mesh in the particle simulation method, crack generation in brittle materials can be modeled in a much easier and flexible manner. For example, if a normal contact force exceeds the corresponding normal tensile bond strength at a contact between two particles or between a particle and a boundary, the normal tensile bond is broken and therefore, a tensile crack, which is equivalent to Mode I crack in the conventional fracture mechanics sense, is generated at the contact. Similarly, if a shear contact force exceeds the corresponding shear bond strength at a contact between two particles or between a particle and a boundary, the tangential shear bond is broken and therefore, a shear crack, which is equivalent to Mode II or Mode III crack in the conventional fracture mechanics sense, is generated at the contact. Secondly, the dynamic process of crack generation can be automatically simulated in the particle simulation method. This means that the subcritical crack growth mechanism, which is often difficult to simulate in the conventional finite element method with automatic re-meshing algorithms (Zienkiewicz and Zhu, 1991; Bouchard et al., 2003), can be modeled using the particle simulation method. Thirdly, because only one particle is contributed to the "global" matrix of the system in the particle simulation method, a significant reduction in the requirement for computer memory can be made during every step of the simulation. Fourthly, multi-scale phenomena can be simulated in a relatively simple manner. For example, by allowing a particle to be split into several smaller particles, particle collapsing phenomena can be automatically simulated. By joining several particles together, massive conglomeration phenomena of particles can also be simulated.

3. Effects of loading rates and particle size on mechanical response of a particle system using the discontinuous loading procedure

Since both the time-scale and the length-scale are significantly different between engineering problems and geological ones, it is necessary to deal with an upscale issue when the particle simulation method is applied to simulate geological systems. An important aspect of the upscale issue is how to correctly use the rock mechanical property measured from a laboratory experiment to simulate the mechanical response of crustal rocks using the particle simulation method. Because the particle-scale mechanical properties of materials, such as the particle stiffness and bond strength, are used in particle simulation models but they are not known *a priori*, it is important to deduce these particle-scale mechanical properties of materials from the related macroscopic ones measured from both laboratory and field experiments. This means that an inverse problem needs to be solved through the numerical simulation of a particle system. For such an inverse problem, input parameters are the macroscopic mechanical properties of materials, while the particle-scale mechanical properties of materials, such as the particle stiffness and bond strength, are unknown variables and therefore, need to be determined (Zhao et al., 2007b). In geological practice, a kilometer-length-scale specimen is often used to conduct a biaxial compression test and to measure the related macroscopic mechanical properties, such as the elastic modulus and material strength, from the mechanical response of the particle model having an assumed set of particle-scale mechanical properties of rocks. However, if some mechanical properties are independent of particle size or other size-dependent mechanical properties may be determined from an appropriate upscale rule, then the expected particle-scale mechanical properties of materials to be used in a particle model can be determined without a need to conduct the trial-and-error exercise (Wang et al., 2000; Griffiths and Mustoe, 2001). From this point of view, it is necessary to investigate the effect of both the loading rate and the particle size on the mechanical response of a particle model through conducting a series of biaxial compression tests in this section.

As shown in Fig. 3, two samples of different sizes are considered in the particle simulation tests. The first test sample is of a small size of 1 by 2 m and simulated using 100 and 1000 particles respectively. When the small test sample is simulated using 100 particles, the maximum and minimum radii of particles are approximately 0.0545 m and 0.0363 m, resulting in an average radius of 0.0454 m. However, when the small test sample is simulated using 1000 particles, the maximum and minimum radii of particles are approximately 0.0172 m

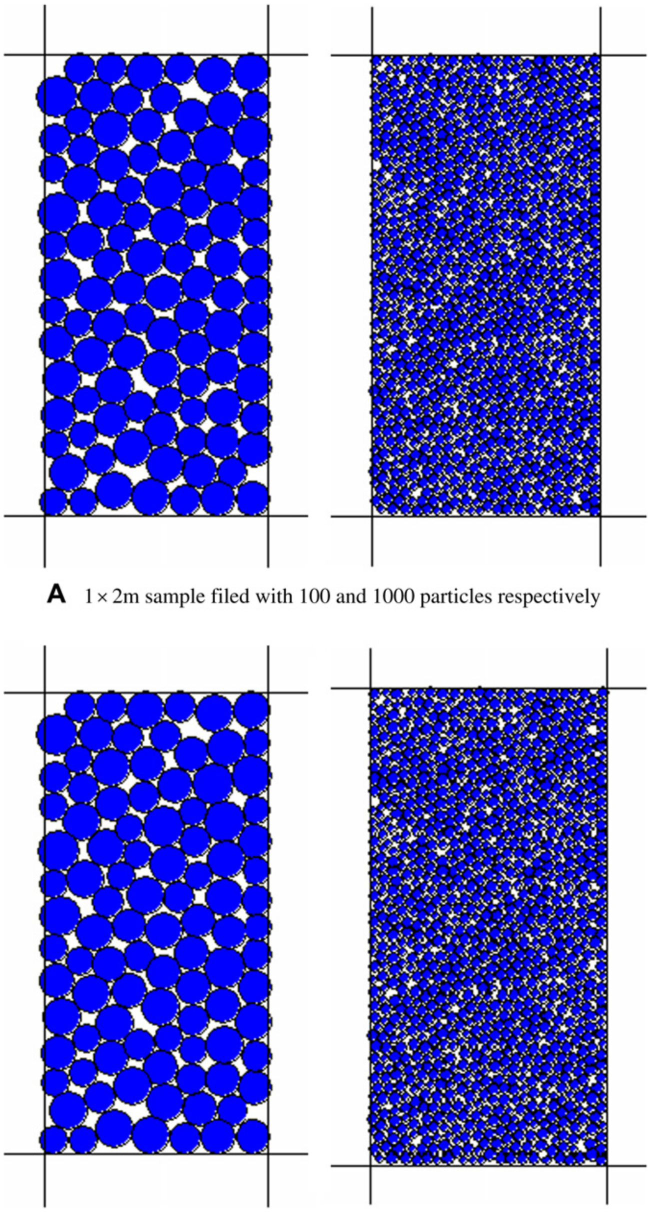

A 1×2m sample filed with 100 and 1000 particles respectively

B 1×2km sample filed with 100 and 1000 particles respectively

Fig. 3. Initial geometrical shapes of the samples used in the numerical test.

and 0.0115 m, resulting in an average radius of 0.0144 m. On the contrary, the second test sample is of a large size of 1 by 2 km and also simulated using 100 and 1000 particles. In the case of the large test sample of 100 particles, the maximum and minimum radii of particles are approximately 54.52 m and 36.35 m, resulting in an average radius of 45.43 m, while in the case of 1000 particles, the maximum and minimum radii of particles are approximately 17.24 m and 11.49 m, resulting in an average radius of 14.37 m. The porosity of both the small and the large test samples is set to be 0.17 in the particle simulation. The confining stress is assumed to be 10 MPa in the following numerical experiments. The density of the particle material is 2500 kg/m^3 and the friction coefficient of the particle material is 0.5. It is noted that since this investigation is focused on the particle simulation of quasi-static problems, the friction coefficient of the particle material is assumed to be constant and independent of time in this investigation. However, if one is interested in the application of the particle simulation method to seismological problems, then the time-dependent friction laws (e.g. Dieterich, 1978; Ruina, 1983; Bizzarri et al., 2001) should be used in the simulation. Due to a significant size difference between the small and large test samples, the size effect of the test sample can be investigated through the particle simulation.

The stiffness and bond strength of particles in a test sample can be predicted using the macroscopic mechanical properties such as the elastic modulus, tensile and shear strength of particle materials. From the analog of a two-circle contact with an elastic beam (Itasca Consulting Group Inc., 1999), it has been demonstrated that there may exist an upscale rule, which states that the contact stiffness of a circular particle is only dependent on the macroscopic elastic modulus and independent of the diameter of the circular particle. The value of the contact stiffness of a circular particle is equal to twice that of the macroscopic elastic modulus of the material. On the other hand, the contact bond strength of a circular particle is directly proportional to both the tensile/shear strength of the particle material and the diameter of the circular particle. Keeping the above considerations in mind, the following macroscopic mechanical properties of rock masses are used to determine the contact mechanical properties of the particle material used in the simulation. The macroscopic elastic modulus of the particle material is 0.5 GPa, resulting in the contact stiffness (in both the normal and the tangential directions) of 1.0 GN/m for each particle in both the small and the large test samples. The macroscopic tensile strength of the particle material is 10 MPa, while the macroscopic shear strength of the particle material is 100 MPa for both the small and the large test samples. Damping is used so that an equilibrium state can be reached in the particle simulation.

The robustness of the discontinuous loading procedure can be examined by the simulation-solution independence of the loading rate, which is the fundamental characteristic of a quasi-static problem. As usual, the servo-control technique (Itasca Consulting Group Inc., 1999) is used to apply the equivalent velocity of applied stresses or forces to the loading boundary of the particle model. The equivalent velocity is called the loading rate hereafter. Fig. 4 shows the effect of the loading rate on the curve of deviatoric stress versus axial strain for both the small and the large samples of 1000 particles. Fig. 5 displays the effect of the loading rate on the curve of volumetric strain versus axial strain, while Fig. 6 shows the effect of the loading rate on the curve of confining stress versus axial strain. It is obvious that the simulated stress-strain curve and volumetric-axial strain curve are independent of the two loading rates (i.e. LR = 1 m/s and LR = 10 m/s in this figure) within the elastic response range of the test material (i.e. before the occurrence of the first crack within the test sample). It can be found, from the stress-strain curve, that the simulated elastic modulus of the particle material is equal to 0.5 GPa, which is identical to the desired value of the expected

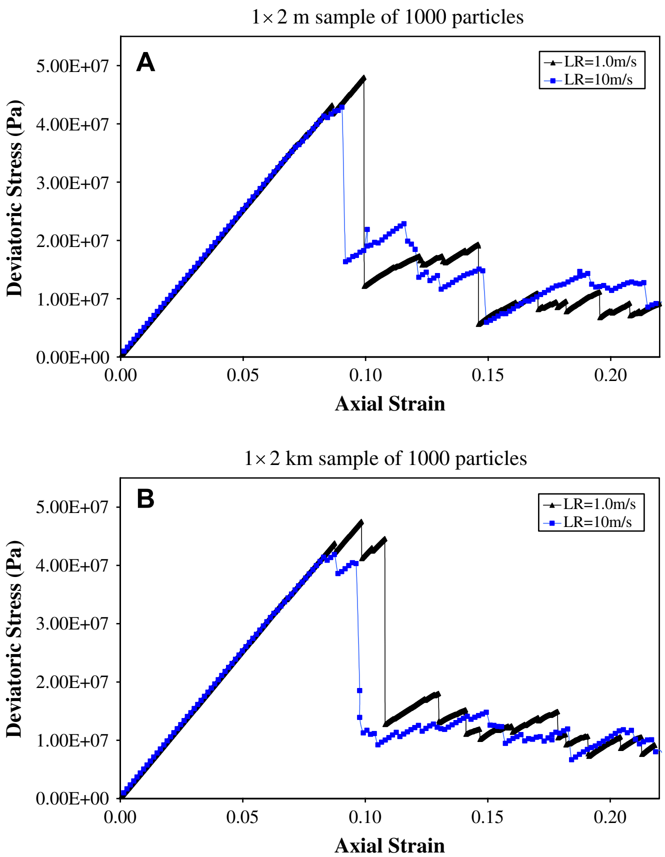

Fig. 4. Effects of loading rate on the curve of deviatoric stress versus axial strain. LR is the loading rate applied to the test sample.

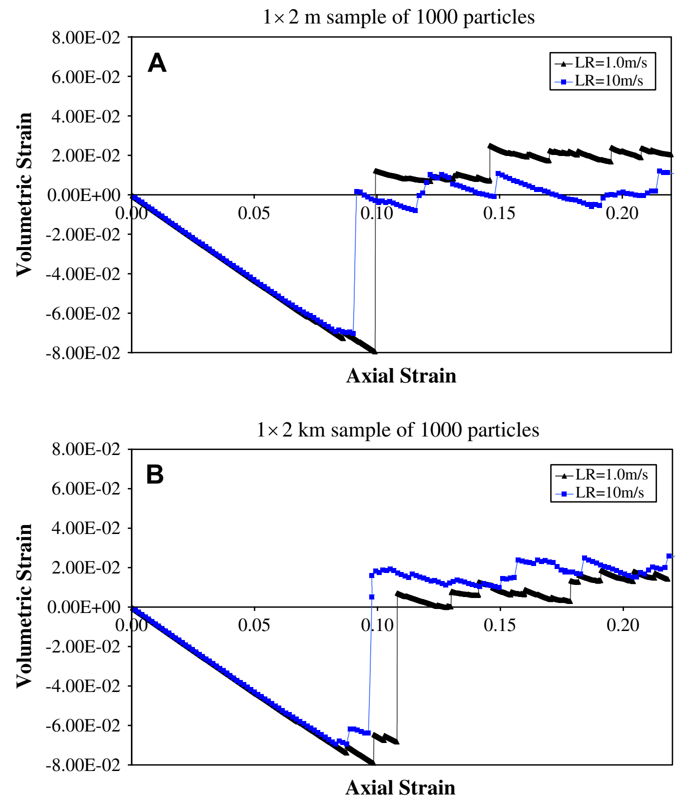

Fig. 5. Effects of loading rate on the curve of volumetric strain versus axial strain. LR is the loading rate applied to the test sample.

macroscopic elastic modulus of the particle material. This indicates that the upscale rule established from the analog of a two-circle contact with an elastic beam (Itasca Consulting Group Inc., 1999) is appropriate for predicting the elastic modulus when the discontinuous loading procedure is used in the simulation of a particle model.

After the deviatoric stress, which is defined as axial stress minus confining stress, reaches its maximum value (i.e. the yielding strength) at an axial strain of about 10%, the mechanical responses of these two different length-scale samples are different, indicating that once the major failure occurs, the mechanical response of the particle sample is strongly non-linear and dependent on both the loading rate and the particle size. In the case of the small-size sample of 1000 particles, the average size of particles is small enough to capture the major microscopic seismicity that occurs during any major failure process of the sample. As shown in Fig. 4A, there are three major failures occurring at the axial strain of about 10%, 14% and 19% respectively. These major failures can cause a considerable amount of elastic energy release so that they have an impact on the confining stress applied to the lateral boundaries of the sample. This phenomenon is clearly recorded in the confining stress versus axial strain curve shown in the small-size model of 1000 particles (see Fig. 6A).

Although the linear elastic behavior of both the small and the large test samples of 1000 particles is independent of the sample size, particle size and loading rate, it may be dependent on the total number of particles used in a particle simulation. If the total number of particles in a particle simulation is too small, the macroscopic behavior of the particle system may not be appropriately simulated because of the poor resolution of the simulation results. This issue can be investigated through conducting biaxial compression tests of both the small and the large test samples of 100 particles (see Fig. 3). Fig. 7 shows the effect of the total particle number on the curve of deviatoric stress versus axial strain for both the small and the large test samples of 100 particles. Fig. 8 displays the effect of the total particle number on the curve of volumetric strain versus axial strain, while Fig. 9 shows the effect of the total particle number on the curve of confining stress versus axial strain for both the small and the large test samples of 100 particles. It is noted that even though 100 particles are only used to simulate both the small (i.e. 1 by 2 m) and the large (i.e. 1 by 2 km) test samples, the linear elastic behavior of these two test samples (before the occurrence of the first crack within the test samples) remains independent of the sample size, particle size and loading rate in the case of using the discontinuous loading procedure to conduct biaxial compression tests. By comparing the simulation results obtained from 100-particle samples (see Figs. 7–9) with those obtained from 1000-particle samples (see Figs. 4–6), it is recognized that although the maximum yielding strength is of the same order of magnitude for all the simulation results, there is a considerable failure (see Fig. 7) in the 100-particle samples before

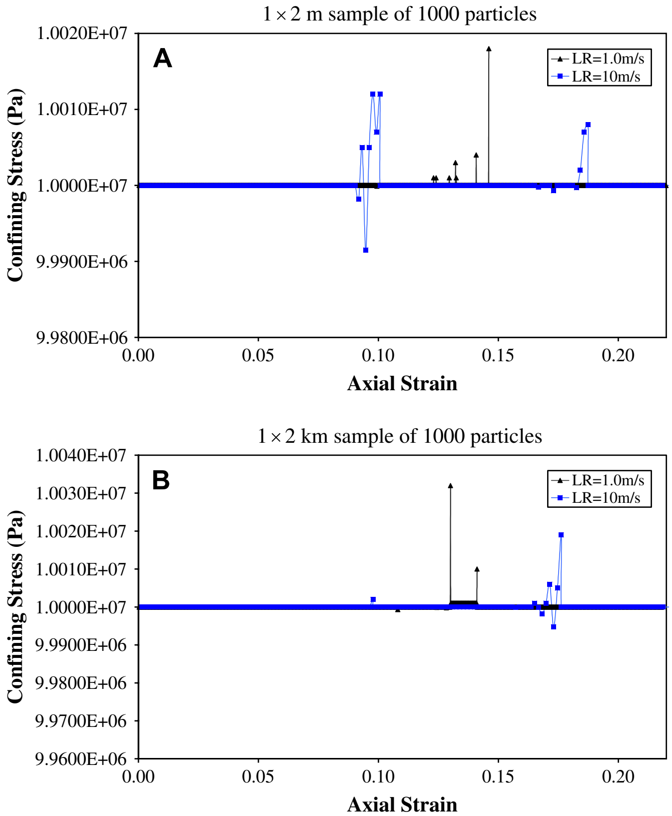

Fig. 6. Effects of loading rate on the curve of confining stress versus axial strain. LR is the loading rate applied to the test sample.

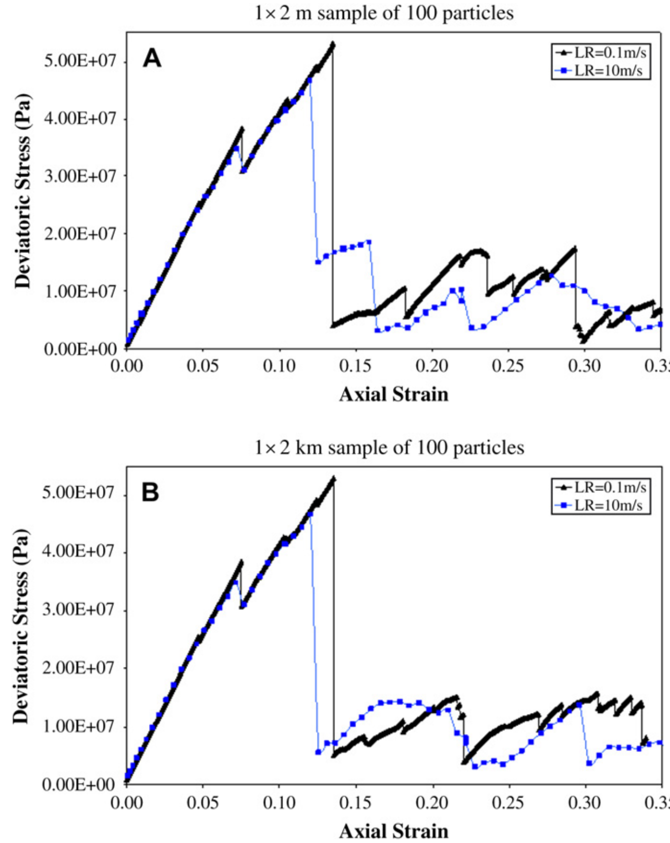

Fig. 7. Effects of the total number of particles on the curve of deviatoric stress versus axial strain. LR is the loading rate applied to the test sample.

their linear elastic response reaches the corresponding maximum yielding strength. This phenomenon indicates that due to the use of a small number of particles, both the 100-particle samples of different sample sizes cannot capture the small-scale and microscopic-scale failure behavior of the particle system. This conclusion can be further confirmed by comparing the simulation results shown in Fig. 9 with those shown in Fig. 6. It is clearly observed that the 100-particle samples of two different sample sizes cannot capture the primary microscopic seismicity that occurs during a primary failure process, which is in correspondence with the biggest drop in the deviatoric stress of the test sample. In theory, the greater the total number of particles is used in a particle simulation, the better the detailed microscopic phenomenon can be captured in the particle model. However, in practice, the greater the total number of particles is used in a particle simulation, the larger the computer efforts are required in the simulation. For this reason, the total number of particles that are used in a particle simulation should be adequate, so that the concerned macroscopic phenomenon in a large-scale geological system can be simulated without wasting any computer efforts. Therefore, it is recommended that the particle-size sensitivity analysis of at least two different models, which have different total number of particles, be carried out to confirm the particle simulation result of a large-scale geological system.

It is worth comparing the particle simulation results obtained from using the discontinuous loading procedure with those obtained from using the continuous loading procedure. For this purpose, both the small and the large test samples of 1000 particles are used to conduct biaxial compression tests using the continuous loading procedure. Fig. 10 shows the effect of the loading rate on the curve of deviatoric stress versus axial strain for both the small and the large test samples of 1000 particles using the continuous loading procedure. It is obvious that the general solution pattern for both the small and the large test samples of 1000 particles is very similar, indicating that the sample size of a particle model has little influence on the mechanical response of the model, even if the continuous loading procedure is used to produce the simulation results. However, the mechanical responses of both the small and the large test samples of 1000 particles are clearly dependent on the loading rate, especially in the case of the loading rate being 10 m/s. For this particular loading rate, as shown in Fig. 4, the mechanical responses of both the small and the large test samples of 1000 particles are independent of the loading rate in the case of using the discontinuous loading procedure. Nevertheless, the loading-rate dependence of the mechanical response obtained from using the continuous loading procedure is greatly reduced when the smaller loading rate (i.e. LR = 1.0 m/s and LR = 0.1 m/s) is used in the particle simulation, indicating that the use of the continuous loading procedure in a particle simulation may produce some useful results as long as the loading rate is kept very small in the particle simulation. In the case of the loading rate being

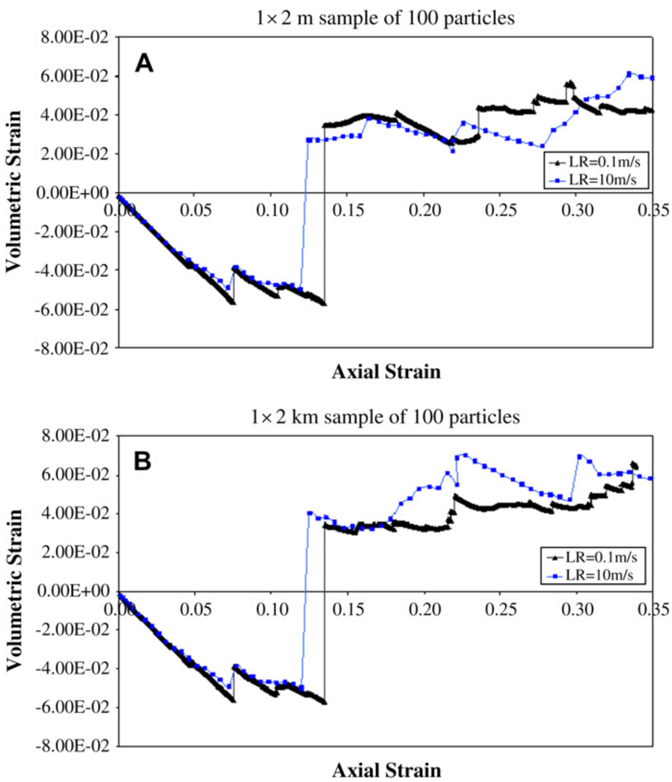

Fig. 8. Effects of the total number of particles on the curve of volumetric strain versus axial strain. LR is the loading rate applied to the test sample.

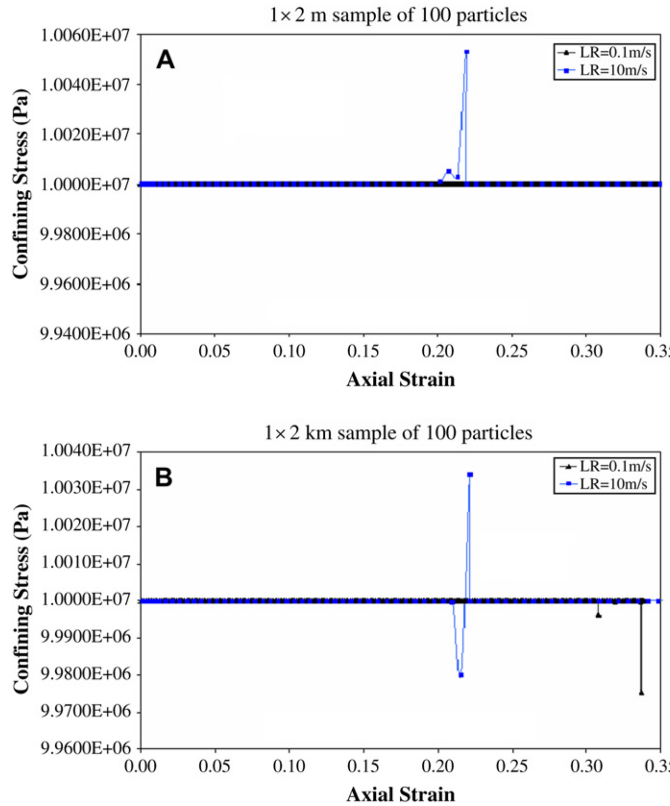

Fig. 9. Effects of the total number of particles on the curve of confining stress versus axial strain. LR is the loading rate applied to the test sample.

10 m/s, the maximum yielding strength obtained from using the continuous loading procedure is almost twice that obtained from using the discontinuous loading procedure, implying that the maximum yielding strength can be overestimated from using the continuous loading procedure. It is interesting to note that the mechanical response obtained from using the continuous loading procedure exhibits the stronger ductile behavior (Fig. 10), while the mechanical response obtained from using the discontinuous loading procedure exhibits the stronger brittle behavior (Fig. 4) for exactly the same test sample. This demonstrates that in addition to the conceptual soundness, the newly-proposed discontinuous loading procedure is more appropriate than the continuous loading procedure in dealing with the numerical simulation of the brittle behavior of crustal rocks.

Since the main purpose of this study is to simulate spontaneously-distributed crack generation in brittle crustal rocks using the particle simulation method, it is important to examine the accuracy of the predicted crack patterns from using the discontinuous loading procedure. In theory, the smallest particle size of a particle simulation model is related directly to the material fracture toughness (Potyondy and Cundall, 2004), especially under mixed compressive-extensile conditions. In the case of modeling damage processes for which macroscopic cracks form, the smallest particle size and model properties should be chosen to match the material fracture toughness as well as the unconfined compressive strength. However, it was also indicated that the formation of a failure plane and secondary macro-cracks may be independent of particle size under mixed compressive-shear conditions (Potyondy and Cundall, 2004). In order to test whether or not the formation of macroscopic cracks is dependent on the smallest particle size, both the small and the large test samples of 1000 particles are used to conduct biaxial compression tests using the discontinuous loading procedure. In the case of the small test sample of 1000 particles, the radius of the smallest particle is 0.0115 m, while in the case of the large test sample of 1000 particles, the radius of the smallest particle is 36.35 m. Fig. 11 shows the effect of the loading rate and particle size on the crack patterns of two different length-scale test samples. These crack patterns are obtained when the axial strain of the test sample is about 35%. It is noted that in the case of either a small test sample of 1 by 2 m or a large test sample of 1 by 2 km, the predicted crack patterns are essentially similar, at least from the phenomenological modeling point of view. This demonstrates that the discontinuous loading procedure is independent of the loading rate, even though it is used to simulate the spontaneously-distributed crack generation in brittle crustal rocks. However, it is obvious that there is a remarkable discrepancy between the two kinds of crack patterns obtained from the small and large test samples, indicating that the smallest particle size used in a particle simulation has a significant influence on the predicted crack pattern of the particle model. Since the particle size-dependent issue cannot be completely removed when we apply the particle simulation method to solve crack generation problems in large-scale geological systems, it is recommended that the

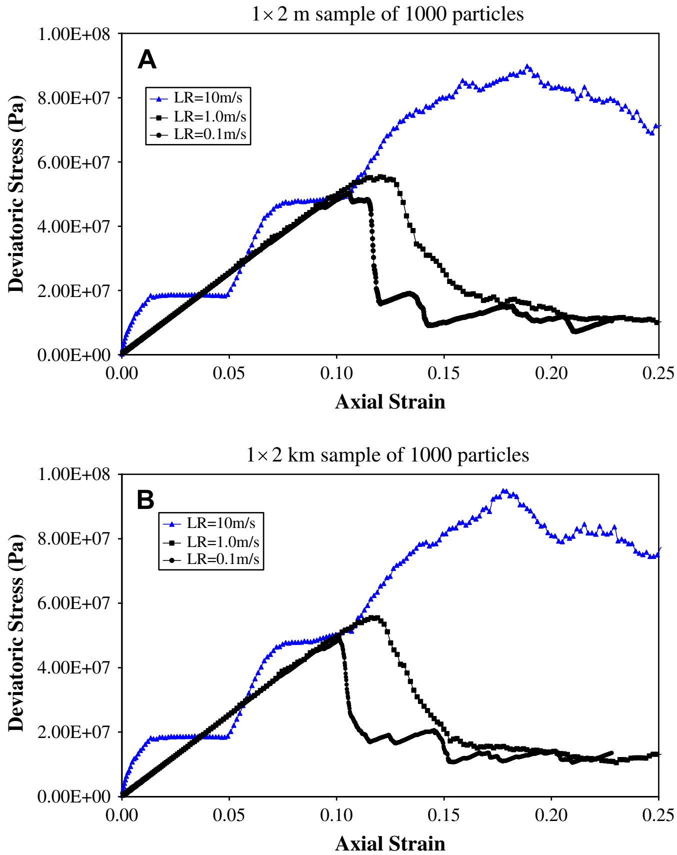

Fig. 10. Effects of loading rate on the curve of deviatoric stress versus axial strain using the continuous loading procedure. LR is the loading rate applied to the test sample.

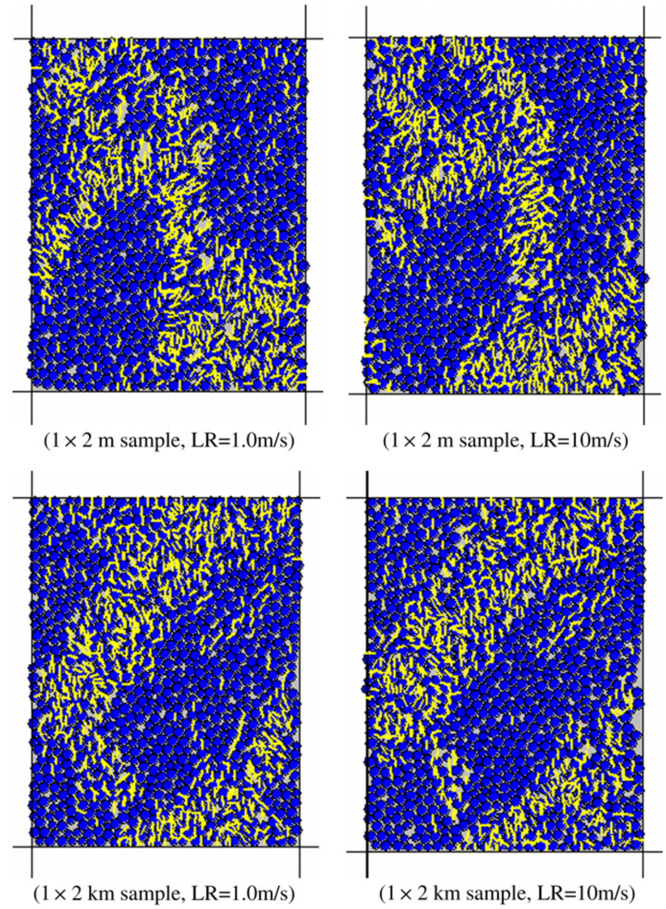

Fig. 11. Effects of loading rate and particle size on crack patterns of two different length-scale samples. LR is the loading rate applied to the test sample.

particle-size sensitivity analysis of at least two different models, which have the same geometry but different smallest particle size, be carried out to confirm the particle simulation result of a large-scale geological system.

4. Phenomenological modeling of spontaneously distributed crack generation in brittle crustal rocks

In order to illustrate the possible application of the particle simulation method combined with the discontinuous loading procedure to large-scale geological problems, the phenomenological modeling of spontaneously distributed crack generation in brittle crustal rocks is carried out in this section. The problem to be considered is related to the basement controlled reverse faulting, resulting in crustal fault-propagation folding above rigid basement blocks. The reason for choosing this kind of problem is that it has been widely investigated for many years (see Finch et al., 2003, 2004, and the references therein). For instance, Finch et al. (2003, 2004) used the distinct element modeling to investigate the mechanical deformation related to the formation and evolution of both the contractional and the extensional fault-propagation folding above rigid basement blocks. For the purpose of justifying the distinct element method for simulating large-scale geological systems, Finch et al. (2003, 2004) compared the particle simulation results with those obtained from both the trishear kinematical model (Erslev, 1991) and field observations. This means that in terms of the mechanical deformation patterns, this kind of problem can be used as a benchmark problem, against which a combination of the particle simulation method and the discontinuous loading procedure can be validated. Although the mechanical deformation patterns related to the formation and evolution of both the contractional and the extensional fault-propagation folding above rigid basement blocks were widely investigated, little, if any, work has been carried out on the particle simulation of spontaneous crack generation for this kind of problem. Therefore, this section is focused on demonstrating the application of the particle simulation method combined with the discontinuous loading procedure to large-scale geological problems through the particle simulation of the spontaneous crack generation caused by the crustal fault-propagation folding above rigid basement blocks.

Fig. 12 shows the geometry of the computational model, in which the length and initial thickness are 10 km and 2.5 km respectively. The dip angle of a pre-existing fault in the rigid basement is 60 degrees (i.e. $\theta = 60°$). The model is simulated by 4000 particles. The maximum and minimum radii of particles are approximately 30.48 m and 20.32 m, resulting in an average radius of 25.4 m. Although the model is mechanically

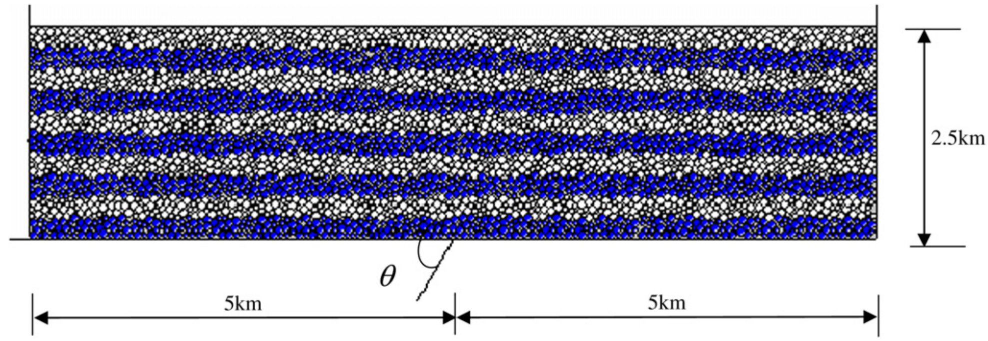

Fig. 12. Geometry of the computational model.

comprised of one homogeneous layer, we use 10 approximately flat-lying and constant-thickness marker beds to monitor the deformation patterns. The macroscopic elastic modulus of the particle material used in the model is 5 GPa, resulting in the contact stiffness (in both the normal and the tangential directions) of 10 GN/m for each particle in the computational model. The macroscopic tensile strength of the particle material is 20 MPa, while the macroscopic shear strength of the particle material is 200 MPa for the computational model. The density of the particle material is assumed to be 2500 kg/m^3 in the particle simulation. Although two vertical boundaries are fixed, particles in contact with them are allowed to move in the vertical direction but not allowed to move in the horizontal direction of the computational model. Since the top of the computational model is a free surface, a stress-free boundary condition is applied to this boundary. In order to simulate the slip of the pre-existing fault, the right half of the bottom is fixed, while the left half of the bottom is

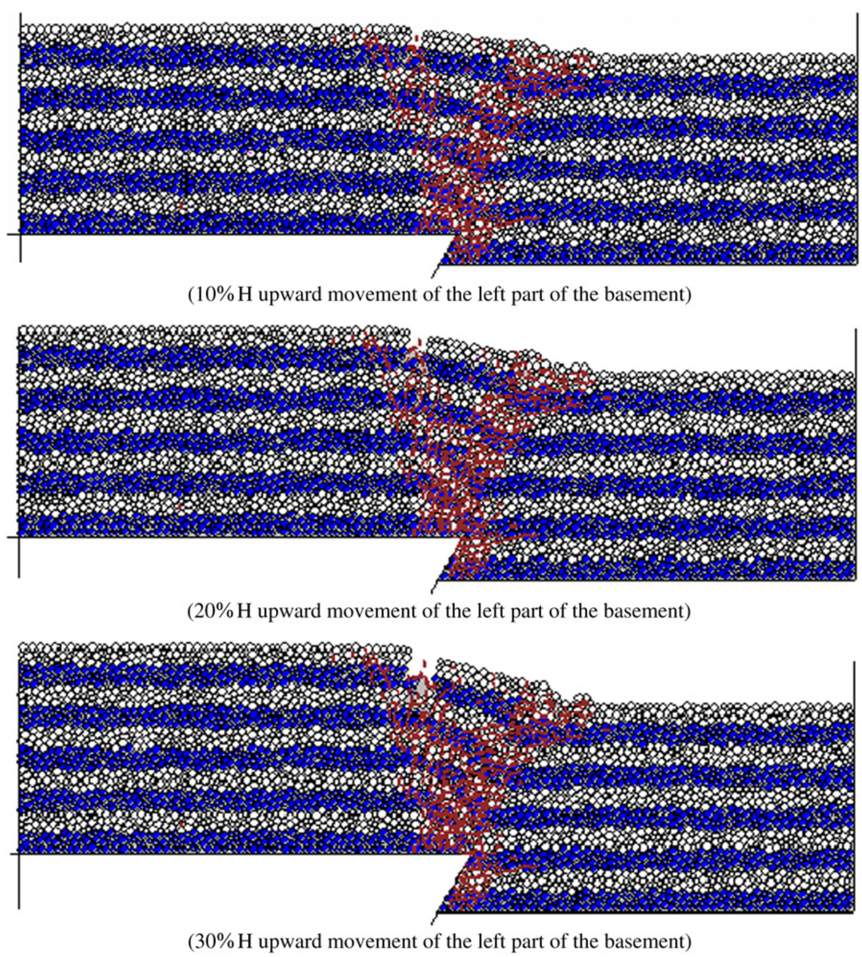

Fig. 13. Crack generation and evolution within the computational model (crack pattern with showing particles). H is the initial thickness of the computational model.

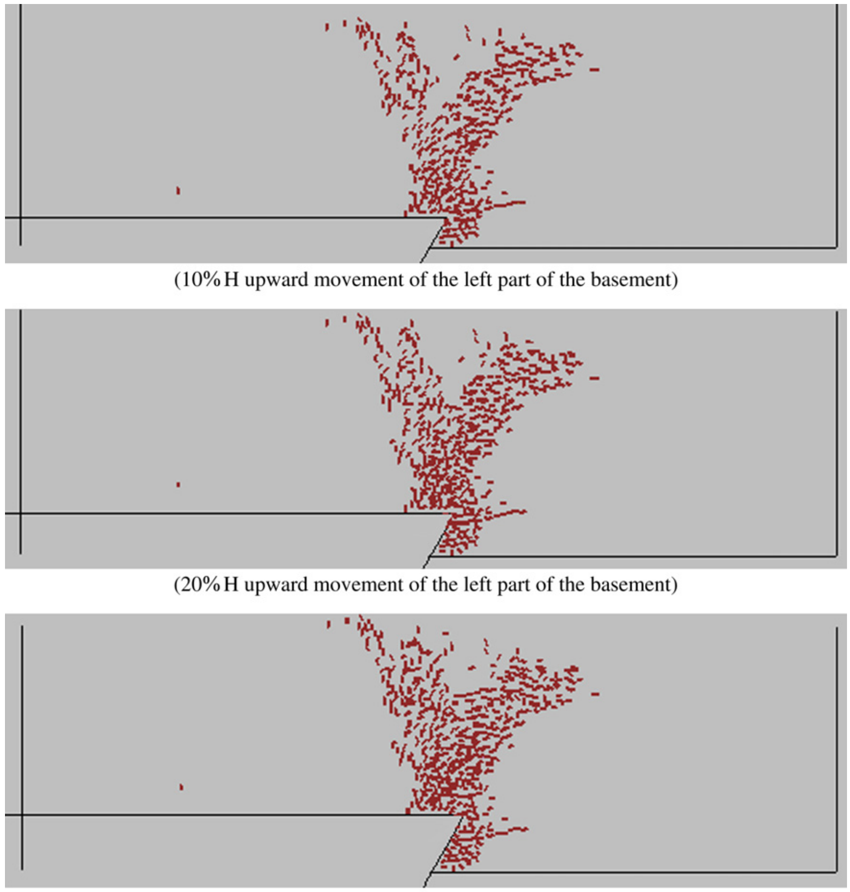

(10% H upward movement of the left part of the basement)

(20% H upward movement of the left part of the basement)

(30% H upward movement of the left part of the basement)

Fig. 14. Crack generation and evolution within the computational model (crack pattern without showing particles). H is the initial thickness of the computational model.

allowed to move in the direction parallel to the pre-existing fault plane within the rigid basement. The gravity effect is considered by running the computational model to reach an initial equilibrium state due to gravity.

Fig. 13 shows the crack generation and evolution process of the computational model at three different stages of 10%H, 20%H and 30%H upward movement of the left part of the basement, where H is the initial thickness of the computational model. In order to display the crack pattern clearly, the particles shown in Fig. 13 are removed so that only the crack pattern is shown in Fig. 14. From the simulation results shown in these two figures, it is observed that two major macroscopic cracks are generated as a result of many small-scale cracks being linked together. There is a triangle zone between these two major macroscopic cracks. Although one major macroscopic crack is generated along the slip direction of the pre-existing fault in the rigid basement, the other major macroscopic crack is clearly generated within the hangingwall of the simulated brittle upper crust. It is noted that the deformation pattern displayed in Fig. 13 is very similar to that reported in the previous publication by Finch et al. (2003). Since Finch et al. (2003, 2004) compared the particle simulation results with those obtained from both the trishear kinematical model (Erslev, 1991) and field observations, it has demonstrated that in addition to the conceptual soundness, the discontinuous loading procedure is correct and useful for dealing with the numerical simulation of the brittle behavior of crustal rocks.

In order to compare the predicted crack pattern from using the discontinuous loading procedure with that from using the continuous loading procedure, the same computational model was rerun using the continuous loading procedure. Fig. 15 shows the comparison of crack patterns due to two different loading procedures. The crack patterns shown in this figure are generated when the vertical component of the slip of the pre-existing fault is about 30% initial thickness of the computational model. It is observed that there are some significant differences between the simulation results obtained from using two different loading procedures. For example, a large crack is generated in the top two marker beds in the case of using the discontinuous loading procedure in the particle simulation, but this phenomenon cannot be observed in the case of using the continuous loading procedure. In addition, the microscopic cracks are more diffusely distributed within the hangingwall when the continuous loading procedure is used in the particle simulation. The reason for these differences is that the use of the continuous loading procedure may exaggerate the ductile behavior of brittle rocks and therefore, the continuous loading procedure is not appropriate for simulating the brittle behavior

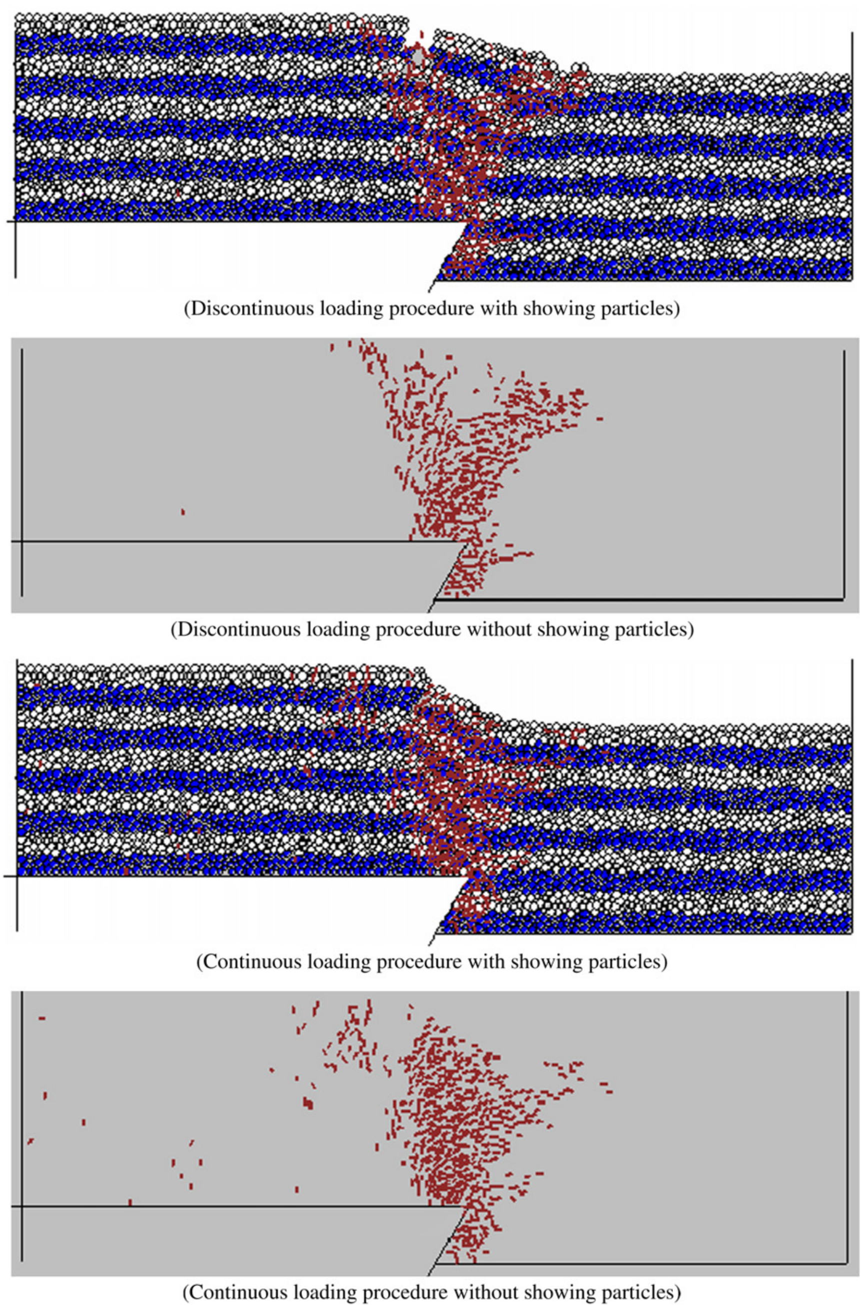

Fig. 15. Comparison of crack patterns due to two different loading procedures.

of crustal rocks in a particle simulation. On the contrary, the use of the discontinuous loading procedure can correctly represent the brittle behavior of brittle rocks, as mentioned in the previous sections. For this reason, the newly-proposed discontinuous loading procedure is more suitable for simulating spontaneously-distributed crack generation in brittle crustal rocks.

5. Conclusions

The particle simulation method has been successfully used to simulate spontaneous crack generation in large-scale geological systems. Since both the time-scale and the length-scale are quite different between laboratory specimens and geological systems, it is necessary to deal with an upscale issue when the particle simulation method is applied to solve geological problems. If a geological system can be treated as a quasi-static one, then the mechanical response of the system should be independent of the loading rate. Based on this understanding, we have examined the continuous type of loading procedure that is commonly used in PFC2D and a newly-proposed discontinuous type of loading procedure, which is independent of the loading rate, particle size and sample size, especially in the elastic response range of a particle system. The use of the discontinuous type of loading procedure enables the macroscopic elastic modulus of a two-dimensional particle system to be directly evaluated from the mechanical properties of a particle without a need to conduct biaxial compression tests. However, the particle size-dependent issue cannot be completely removed when the particle simulation method is applied to solve crack generation problems in geological systems. It is possible to deal with this issue through particle-size sensitivity analyses of at least two different models.

Due to the easy consideration of displacement discontinuities at a contact between two particles, the formulation based on the discrete particle simulation is conceptually simpler than that based on the continuum mechanics, because crack generation at a contact between two particles is a natural part of the particle simulation process. The major advantage in using the particle simulation method is that since there is no mesh in the particle simulation method and the interaction between particles is explicitly expressed by the contact force/displacement, crack generation in brittle materials can be modeled in a much easier and explicit manner.

The related results obtained from the particle simulation of biaxial compression tests have demonstrated that the linear elastic response of a two-dimensional particle model is independent of the sample size, particle size and loading rate, but it may be dependent on the total number of particles used in the particle simulation. Therefore, it is recommended that the particle-size sensitivity analysis of at least two different models, which have the same geometry but different smallest particle sizes, be carried out to confirm the particle simulation result of a large-scale geological system.

The continuous type of loading procedure may exaggerate the ductile behavior of brittle rocks so that it is not appropriate for simulating the brittle behavior of crustal rocks in a particle simulation. On the contrary, the newly-proposed discontinuous type of loading procedure can correctly simulate the brittle behavior of crustal rocks. Thus, the newly-proposed discontinuous type of loading procedure is more suitable for simulating spontaneously-distributed crack generation in brittle crustal rocks. Through the phenomenological modeling of a spontaneously-distributed crack generation problem, which is caused by the formation and evolution of basement controlled reverse faulting, it has been demonstrated that the particle simulation method is useful and applicable for simulating spontaneous crack generation phenomena at geological length scales.

Acknowledgements

The authors express their thanks to the anonymous referees for their valuable comments, which led to a significant improvement over an early version of the paper. The authors also thank Dr T.G. Blenkinsop at James Cook University for his encouragement in revising the paper.

References

Antonellini, M.A., Pollard, D.D., 1995. Distinct element modeling of deformation bands in sandstone. Journal of Structural Geology 17, 1165–1182.

Bardet, J.P., Proubet, J., 1992. The structure of shear bands in idealized granular materials. Applied Mechanics Review 45, 118–122.

Bizzarri, A., Cocco, M., Andrews, D.J., Boschi, E., 2001. Solving the dynamic rupture problem with different numerical approaches and constitutive laws. Geophysics Journal International 144, 656–678.

Bouchard, P.O., Bay, Y., Chastel, Y., 2003. Numerical modelling of crack propagation: automatic remeshing and comparison of different criteria. Computer Methods in Applied Mechanics and Engineering 192, 3887–3908.

Burbidge, D.R., Braun, J., 2002. Numerical models of the evolution of accretionary wedges and fold-and-thrust belts using the distinct-element method. Geophysics Journal International 148, 542–561.

Camborde, F., Mariotti, C., Donze, F.V., 2000. Numerical study of rock and concrete behavior by distinct element modeling. Computers and Geotechnics 27, 225–247.

Cundall, P.A., 2001. A discontinuous future for numerical modelling in geomechanics? Proceedings of the Institution of Civil Engineers: Geotechnical Engineering 149, 41–47.

Cundall, P.A., Strack, O.D.L., 1979. A discrete numerical model for granular assemblies. Geotechnique 29, 47–65.

Delenne, J.V., Youssoufi, M.S.E., Cherblanc, F., Benet, J.C., 2004. Mechanical behaviour and failure of cohesive granular materials. International Journal for Numerical and Analytical Methods in Geomechanics 28, 1577–1594.

Dieterich, J.H., 1978. Time-dependent friction and the mechanics of stick slip. Pure Applied Geophysics 116, 790–806.

Donze, F., Magnier, S.A., Bouchez, J., 1996. Numerical modeling of a highly explosive source in an elastic-brittle rock mass. Journal of Geophysical Research 101, 3103–3112.

Erslev, E.A., 1991. Trishear fault-propagation folding. Geology 19, 617–620.

Finch, E., Hardy, S., Gawthorpe, R., 2003. Discrete element modeling of contractional fault-propagation folding above rigid basement fault blocks. Journal of Structural Geology 25, 515–528.

Finch, E., Hardy, S., Gawthorpe, R., 2004. Discrete element modeling of extensional fault-propagation folding above rigid basement fault blocks. Basin Research 16, 489–506.

Griffith, A.A., 1920. The phenomena of rupture and flow in solids. Philosophical Transactions of the Royal Society of London 211, 163–197.

Griffiths, D.V., Mustoe, G.G.W., 2001. Modelling of elastic continua using a grillage of structural elements based on discrete element concepts. International Journal for Numerical Methods in Engineering 50, 1759–1775.

Hazzard, J.F., Young, R.P., 2000. Simulating acoustic emissions in bonded-particle models of rock. International Journal of Rock Mechanics and Mining Sciences 37, 867–872.

Hazzard, J.F., Young, R.P., Maxwell, S.C., 2000. Micromechanical modeling of cracking and failure in brittle rocks. Journal of Geophysical Research 105, 16683–16697.

Imber, J., Tuckwell, G.W., Childs, C., Walsh, J.J., Manzocchi, T., Heath, A.E., Bonson, C.G., Strand, J., 2004. Three-dimensional distinct element modeling of relay growth and breaching along normal faults. Journal of Structural Geology 26, 1897–1911.

Inglis, C.E., 1913. Stresses in a plate due to the presence of cracks and sharp corners. Proceedings of the Institution of Naval Architects 60, 219–241.

Irwin, G.R., Washington, D.C., 1957. Analysis of stresses and strains near the end of a crack traversing a plate. Journal of Applied Mechanics, 361–364.

Itasca Consulting Group, Inc, 1999. Particle Flow Code in Two Dimensions (PFC2D). Minnesota, USA, Minneapolis.

Iwashita, K., Oda, M., 2000. Micro-deformation mechanism of shear banding process based on modified distinct element method. Powder Technology 109, 192–205.

Klerck, P.A., Sellers, E.J., Owen, D.R.J., 2004. Discrete fracture in quasi-brittle materials under compressive and tensile stress states. Computer Methods in Applied Mechanics and Engineering 193, 3035–3056.

McBride, A., Govender, I., Powell, M., Cloete, T., 2004. Contributions to the experimental validation of the discrete element method applied to tumbling mills. Engineering Computations 21, 119–136.

Owen, D.R.J., Feng, Y.T., de Souza Neto, E.A., Cottrell, M.G., Wang, F., Andrade-Pires, F.M., Yu, J., 2004. The modelling of multi-fracturing solids and particular media. International Journal for Numerical Methods in Engineering 60, 317–339.

Potyondy, D.O., Cundall, P.A., 2004. A bonded-particle model for rock. International Journal of Rock Mechanics and Mining Sciences 41, 1329–1364.
Ruina, A.L., 1983. Slip instability and state variable friction laws. Journal of Geophysical Research 88, 10359–10370.
Saltzer, S.D., Pollard, D.D., 1992. Distinct element modeling of structures formed in sedimentary overburden by extensional reactivation of basement normal faults. Tectonics 11, 165–174.
Schubert, W., Khanal, M., Tomas, J., 2005. Impact crushing of particle-particle compounds: experiment and simulation. International Journal of Mineral Processing 75, 41–52.
Scott, D.R., 1996. Seismicity and stress rotation in a granular model of the brittle crust. Nature 381, 592–595.
Strayer, L.M., Huddleston, P.J., 1997. Numerical modeling of fold initiation at thrust ramps. Journal of Structural Geology 19, 551–566.
Strayer, L.M., Suppe, J., 2002. Out-of-plane motion of a thrust sheet during along-strike propagation of a thrust ramp: a distinct-element approach. Journal of Structural Geology 24, 637–650.
Wang, Y.C., Yin, X.C., Ke, F.J., Xia, M.F., Peng, K.Y., 2000. Numerical simulation of rock failure and earthquake process on mesoscopic scale. Pure Applied Geophysics 157, 1905–1928.
Zhao, C., Hobbs, B.E., Mühlhaus, H.B., 1998. Finite element modelling of temperature gradient driven rock alteration and mineralization in porous rock masses. Computer Methods in Applied Mechanics and Engineering 165, 175–186.
Zhao, C., Hobbs, B.E., Mühlhaus, H.B., Ord, A., Lin, G., 2003. Finite element modeling of three-dimensional steady-state convection and lead/zinc mineralization in fluid-saturated rocks. Journal of Computational Methods in Science and Engineering 3, 73–89.
Zhao, C., Hobbs, B.E., Hornby, P., Ord, A., Peng, S., 2006a. Numerical modelling of fluids mixing, heat transfer and non-equilibrium redox chemical reactions in fluid-saturated porous rocks. International Journal for Numerical Methods in Engineering 66, 1061–1078.
Zhao, C., Nishiyama, T., Murakami, A., 2006b. Numerical modelling of spontaneous crack generation in brittle materials using the particle simulation method. Engineering Computations 23, 566–584.
Zhao, C., Hobbs, B.E., Ord, A., Hornby, P., Peng, S., Liu, L., 2007a. Mineral precipitation associated with vertical fault zones: the interaction of solute advection, diffusion and chemical kinetics. Geofluids 7, 13–18.
Zhao, C., Hobbs, B.E., Ord, A., Hornby, P., Peng, S., Liu, L., 2007b. Particle simulation of spontaneous crack generation problems in large-scale quasi-static systems. International Journal for Numerical Methods in Engineering 69, 2302–2329.
Zienkiewicz, O.C., Zhu, J.Z., 1991. Adaptivity and mesh generation. International Journal for Numerical Methods in Engineering 32, 783–810.